

**Effect of wind speed on the size distribution of gel particles
in the sea surface microlayer: Insights from a wind wave
channel experiment**

Cui-Ci Sun^{1,2,3}, Martin Sperling¹, Anja Engel¹

[1]GEOMAR Helmholtz Centre for Ocean Research Kiel, 24105 Kiel, Germany

[2]State Key Laboratory of Tropical Oceanography, South China Sea Institute of Oceanology,
Chinese Academy of Sciences, 510301, Guangzhou, China

[3]Daya Bay Marine Biology Research Station, Chinese Academy of Sciences, 518000,
Shenzhen, China,

Correspondence to: Anja Engel (aengel@geomar.de)

Running title: variation of gel particles in the SML as a function of wind speed

Key words: wind speed, biogenic gel particle, size distribution, air-sea interface,

Abstract

Gel particles, such as transparent exopolymer particles (TEP) and Coomassie stainable particles (CSP), are important organic components in the sea-surface microlayer (SML). Here, we present results on the effect of different wind speeds on the accumulation and size distribution of TEP and CSP during a wind wave channel experiment in the Aeolotron. Total areas of TEP (TEP_{SML}) and CSP (CSP_{SML}) in the surface microlayer were exponentially related to wind speed. At wind speeds $< 6\text{ms}^{-1}$, accumulation of TEP_{SML} and CSP_{SML} occurred, decreasing at wind speeds of $> 8\text{ms}^{-1}$. Wind speeds $> 8\text{ms}^{-1}$ also significantly altered the size distribution of TEP_{SML} in the 2-16 μm size range towards smaller sizes. The response of the CSP_{SML} size distribution to wind speed varied through time depending on the biogenic source of gels. Wind speeds $> 8\text{ms}^{-1}$ decreased the slope of CSP_{SML} size distribution significantly in the absence of autotrophic growth. For the slopes of TEP and CSP size distribution in the bulk water, no significant difference was observed between high and low wind speeds. Changes in spectral slopes between high and low wind speed were higher for TEP_{SML} than for CSP_{SML}, indicating that the impact of wind speed on size distribution of gel particles in the SML may be more pronounced for TEP than for CSP, and that CSP_{SML} are less prone to aggregation during the low wind speeds. Addition of an *E. huxleyi* culture resulted in a higher contribution of submicron gels (0.4-1 μm) in the SML at higher wind speed ($> 6\text{ms}^{-1}$), indicating that phytoplankton growth may potentially support the emission of submicron gels with sea spray aerosol.

1 **1 Introduction**

2 Two kinds of gel particles have been widely studied in aquatic environments: transparent
3 exopolymer particles (TEP), which include acidic polysaccharides, and Coomassie stainable
4 particles (CSP) that are protein-containing particles and can serve as a N source for bacteria
5 and other organisms (Alldredge et al., 1993;Long and Azam, 1996;Passow, 2002;Engel et al.,
6 2004). A major source of TEP and CSP in the ocean are phyto- and bacterioplankton
7 (Alldredge et al., 1993;Long and Azam, 1996;Stoderegger and Herndl, 1999). Previous
8 studies highlighted the importance of gels for increasing gelatinous biofilm formation in the
9 surface microlayer (Wurl and Holmes, 2008;Cunliffe et al., 2013) and mediating vertical
10 organic matter transport, either up to the atmosphere or down to the deep ocean (Azetsu-Scott
11 and Niven, 2005;Ebling and Landing, 2015;Guasco et al., 2014;Mari et al., 2017). In addition,
12 it has been suggested that gels play an important role in air-sea exchange processes. Gel
13 particles with a polysaccharidic composition ejected by bubble bursting events may act as
14 cloud condensation nuclei (CCN) in low-level clouds regions (Leck and Bigg, 2005;Russell et
15 al., 2010;Orellana et al., 2011). Also proteinaceous gels and amino acids can be enriched in
16 the SML and in sea-spray aerosols (SSA)(Kuznetsova et al., 2005). Since gel particles with
17 fractal scaling provide a relatively large surface to volume ratio, they are assumed to act as
18 barriers at the interface between air and sea, potentially reducing molecular diffusion rates
19 (Engel and Galgani, 2016). Thus, the enrichment of organic matter, including gels, in the
20 SML could modulate the air-sea gas exchange at low and intermediate winds (Calleja et al.,
21 2009; Mesarchaki et al., 2015; Wurl et al., 2016; Engel and Galgani, 2016).

22 Particle-size distribution (PSD) is a trait description of gel particles that relates to many
23 important processes. It has been demonstrated that marine heterotrophs feed on gel particles
24 within specific size ranges (Mari and Kiorboe, 1996). Bacterial colonization of TEP varies as

1 a function of size (Mari and Kiorboe, 1996;Passow, 2002). Thus, changes in size distribution
2 of gel particles will likely alter food-web structure and dynamics in the ocean and SML.

3 Gel PSD and its variation with biogeochemical and physical processes generally reflect the
4 information about coagulation, break-up, and dissolution as well as on sources and sinks of
5 gels particles, either moving upward into or sinking out of the SML. In addition, the
6 abundance and size of gels in the SML and in subsurface waters may determine their potential
7 fate as CCN in the atmosphere (Orellana et al., 2011).

8 Wind was determined as a principal force that controls accumulation of particulate material in
9 the SML and as the most important variable controlling the air-sea exchange of gas and
10 particles (Liu and Dickhut, 1998;UNESCO, 1985;Frew et al., 2004). The SML is expected to
11 disrupt at higher wind speed, but the threshold wind speed for organic matter enrichment in
12 general, and for specific components in particular, is largely unknown (Liss, 2005). Natural
13 slicks often occur at low wind speeds ($<6 \text{ ms}^{-1}$) typically having wider area coverage for
14 longer time in coastal seas compared to the open-ocean (Romano, 1996). Using different
15 SML sampling methods, such as a Teflon plate, glass plate and Garret screen (Garrett and
16 Duce, 1980), direct relationships between wind speed and SML thickness have been
17 determined. Yet, the influence of wind on SML thickness is not clear; Liu and Dickhut (1998)
18 observed a decrease with wind speed up to 5 m s^{-1} , while Falkowska (1999) determined an
19 increase up to a wind speed of 8 m s^{-1} , beyond which the thickness of the SML began to
20 decrease.

21 TEP enrichment in the SML has been described to be inversely related to wind speed greater
22 than $5\text{-}6 \text{ ms}^{-1}$ (Wurl et al., 2009;Wurl et al., 2011;Engel and Galgani, 2016). One explanation
23 for this is that at higher wind speed, aggregation of solid particles with TEP result in
24 aggregates becoming negatively buoyant and sinking out of the SML. For proteinaceous gels,

Engel and Galgani (2016) observed that their enrichment was not inversely related to wind speed. Yet, an inverse relationship between the slope of the CSP size distribution in the SML and wind speed was observed, indicating larger CSP in the SML at low wind speed. In addition, the dynamics of gel particles in the SML were also affected by other mechanisms that depend on the wind and wave conditions. It is proposed that gel particles formation within the SML is supported by bubble scavenging of DOM in the upper water column (Wurl et al., 2011), because more TEP precursors are lifted up the water-column. Moreover, compression and dilatation of the SML due to capillary waves may increase the rate of polymer collision, subsequently facilitating gel aggregation (Carlson, 1983).

Wurl et al. (2011) provided a conceptual model for the production and fate of TEP in surface waters and the underlying controlling mechanisms. However, due to the lack of observational data, we do not understand well how the size distribution of marine gel particles in the SML varies as a function of wind speed and wave action. Knowledge of the characteristics of gel particles such as abundance, total area and size distribution in the SML, and how they relate to wind speed may improve our understanding of marine primary organic aerosol emission-cloud feedback processes and may help to accurately estimate trace gas fluxes from the ocean to the atmosphere. Here, we assess the dynamics of size distribution of marine gels particles, i.e. TEP and CSP, in the SML in responses to different wind speeds.

2 Methods

2.1 Experimental set up

Effects of different wind speeds on the size distribution of organic gel particles in the SML were studied during the Aeolotron experiment from November 3-28, 2014. 22,000 L of North Atlantic seawater were pumped and collected by the research vessel POSEIDON: including

1 ~14000L collected at 55 m at 64° 4.90' N, 8° 2.03' E and ~8000 L collected on the 22. 09.
2 2014 at 5 m depth near the Island of Sylt in the German Bight, North Sea. The water was
3 pumped into a clean (“food save”) road tanker and unloaded at the wind wave facility
4 Aeolotron the following day and stored in the dark and cool (~10°C) until the start of the
5 experiment. It took 41 days from sampling to start the experiment. The Aeolotron (Heidelberg,
6 Germany) is a large-scale annular wind/wave facility with a total height of 2.4m, and an outer
7 diameter of 10m. The wind speed inside the channel was measured by Pitot tube and
8 anemometer. More detailed description of the facility is given by Nagel et al. (2015). The
9 friction velocity U^* was determined and converted into the value U_{10} as described in Bopp
10 and Jähne (2014), with U_{10} being the equivalent wind speed in ten meters height above the
11 ocean.

12 The experiment started on November 3rd (day1). 7 experiments were conducted on days 2, 4,
13 9, 11, 15, 22 and 24, respectively, with stepwise increase in wind speeds (U_{10}) ranging from
14 1.37 to 18.7 m s⁻¹ as shown in Table 1. At some conditions, data of water velocity were absent,
15 hence no values for U_{10} could be obtained. On experimental days, wind started at about 8:00
16 in the morning and ended at about 20:30 in the evening. The actual wind speeds over the
17 seven experiment days varied a little, but all followed the same strategy of setting shown in
18 the conceptual figure 1. Seawater temperature over the course of the experiment was about
19 $21 \pm 1^\circ\text{C}$. A series of manipulations was carried out during the experiment and are described
20 in more detail in the supplementary materials. On day 20, a seed culture of *Emiliana huxleyi*
21 (cell density: 4.6×10^5 cell ml⁻¹) was added followed by a biogenic SML from a previous
22 experiment on day 21. A pair of SML and Bulk water samples was collected at the end of
23 each wind conditions except for day2 and day4, when the bulk water was collected at the start
24 (morning) and the end (evening) of the experiment. Developments of TEP and CSP in the

SML and the bulk water in the course of the Aeolotron study are shown in the Supplementary Material (Figure S1). Compared to the significant changes of gel particles concentration with wind speed observed in the SML, gel concentration changes with wind speed in the bulk water were much smaller. Thus, overall gel concentration in the bulk water was not sensitive to wind speed changes.

2.2 Sampling

SML samples were collected with a glass plate sampler, made of borosilicate glass with dimensions of 500mm (length) \times 250mm (width) \times 5 mm (thickness) and with an effective surface area of 2000 cm² (considering both sides). For each sample, the glass plate was inserted into the water perpendicular to the surface and withdrawn at a rate of ~ 20 cm sec⁻¹. The sample, retained on the glass because of surface tension, was removed by a Teflon wiper. The water from all dips pooled into one sample. Sample volumes were 210-355ml for SML and 800-1000 ml for bulk water, respectively. Samples were collected into acid cleaned (HCl, 10%) and Milli-Q washed glass bottles. Prior to sampling, both glass plate and wiper were rinsed with Milli-Q water, and intensively rinsed with Aeolotron water in order to minimize their contamination with alien material. The first millilitres of SML sample were used to rinse the bottles and then discarded. The bulk water was sampled from the outlet at the middle-lower part of Aeolotron and collected into acid cleaned (HCl, 10%) and Milli-Q washed glass bottles.

2.3 Analytical methods

Total area, particle numbers and equivalent spherical diameter (d_p) of gel particles were determined by microscopy following Engel (2009). For TEP and CSP, 5 to 30 mL were gently filtered (< 150 mbar) onto 25mm Nuclepore membrane filters (0.4 μ m pore size,

Whatman Ltd.), stained with 1 ml Alcian Blue solution for polysaccharidic gels and 0.5ml Coomassie Brilliant Blue G (CBBG) working solution for proteinaceous gels. The excessive dye was removed by rinsing the filter with Milli-Q water. Blank filters for gel particles were prepared using Milli-Q water. Filters were transferred onto Cytoclear© slides and stored at -20 °C until microscopic analysis. Each treatment had two duplicates. For each filter, about 30 images were randomly taken at ×200 magnification with a light microscope (Zeiss Axio Scope A.1). Image-analysis software (Image J, US National Institutes of Health) was used to analyse particle numbers and area. The total particle abundance and total area were determined from a minimum particles size of 0.4 µm ESD. The submicron gel particles during this study covered a range of 0.4-1µm.

The size-frequency distribution of TEP and CSP gels was described by:

$$\frac{dN}{d(d_p)} = k d_p^\delta \quad (1)$$

where dN is the number of particles per unit water volume in the size range d_p to $(d_p+d(d_p))$ (Mari and Kiorboe, 1996). The factor k is a constant that depends on the total number of particles per volume, and δ ($\delta < 0$) describes the spectral slope of the size distribution. The less negative is δ , the greater is the fraction of larger gels. The process of collision of particle in shear is typically important for particles larger than a few µm in diameter and less important than Brownian motion for particles in the submicron size range (Mccave, 1984), therefore both δ and k were derived from regressions of $\log[dN/d(dp)]$ versus $\log[dp]$ over the size range 2–16µm ESD.

On day 11, samples taken at wind of 1.66 ms⁻¹ and 2.89 ms⁻¹ were contaminated and therefore removed from data analysis and discussion.

2.4 Data analysis

Results from the SML samples were compared to those of bulk water and expressed as enrichment factors (EF), defined as:

$$EF = (C)_{\text{SML}} / (C)_{\text{Bulk}} \quad (2)$$

Where (C) is the concentration of a given parameter in the SML or bulk water, respectively (GESAMP, 1995). Enrichment of a component is generally indicated by $EF > 1$, depletion by $EF < 1$. Considering the measurement uncertainty of gel particles using microscopic method within 10%, EF values > 1.1 thus represent significant enrichment of gel particle in the SML, while $EF < 0.9$ is determined to be a depletion.

Nonparametric statistics (Two Sample-Kolmogorov-Smirnov test) was performed to compare differences of slope of gel particles size distribution between low and moderate wind speeds ($< 8\text{ms}^{-1}$) and high wind speeds ($> 8\text{ms}^{-1}$). In addition, statistical significance of changes with respect to the slope of gel particles size distribution after adding the seed culture of *E. huxleyi* and the biogenic SML water from a previous experiment was determined with two sample-Kolmogorov-Smirnov test on non-normalized anomalies given the data being normal distributed. Average values are given by the statistical mean and its standard deviation (SD). Statistical significance was accepted for $p < 0.05$. Calculations and statistical tests were conducted using Microsoft Office Excel 2010 and Origin 9.0 (OriginLab Corporation, USA) software.

3 Results

3.1 Biological variations during the Aeolotron experiment

Temporal changes in hetero- and autotrophic plankton and neuston abundance and in organic matter during the experiment will be described in more detail elsewhere (Engel et al., 2018) and are summarized here only briefly. Heterotrophic microorganisms dominated cell

abundance and biomass in the tank during the whole study. Two peaks of bacterial abundance in the SML occurred on day 4 and on day 11, respectively. Primary production was low during the whole experiment. Chlorophyll *a* (Chl *a*) concentrations were not detectable until days 20/21, i.e. after the addition of the *E. huxleyi* culture and the SML water from a previous phytoplankton bloom experiment. Chl *a* concentration clearly increased after day 23.

3.2 TEP and CSP abundance and total area variations with respect to wind speeds

Before the onset of the wind experiments, the water surface was flat without visible surface movement. As the wind speed increased, the first capillary waves became visible and started breaking above about $U_{10} = 6 \text{ ms}^{-1}$ (e.g. $U_{10} = 6.1 \text{ ms}^{-1}$ on day 22). At this wind speed, abundance of TEP_{SML} decreased, except for day 15 and day 11, when abundance of TEP_{SML} remained relatively stable or even increased slightly at high wind speed (Fig.2). Similar to TEP_{SML} , abundance and total area of CSP_{SML} decreased with increasing wind speed, excluding day 11 and day 2 (Fig. 3). Exponential declines of total area TEP_{SML} and CSP_{SML} with increasing wind speed were observed, except for TEP_{SML} area on day 11 and day 15, and CSP_{SML} area on day 15; a measure of the goodness of exponential fit is the coefficient of determination (COD) denoted as r^2 yielding $r^2_{\text{CSP-Totalarea}} = 0.73 \pm 0.20$, $n=6$ and $r^2_{\text{TEP-Totalarea}} = 0.87 \pm 0.19$, $n=5$. In contrast to total area, only 3 out of 7 observations for abundance of TEP_{SML} and 2 out of 7 for abundance of CSP_{SML} were exponentially related to wind speed. Thus, the relationship between abundance of gel particles in the SML and wind speeds could not be well described by an exponential function. Nevertheless, the reduction of gel particles abundance and area in the SML indicated a clear removal from the SML with increasing wind speed. Enrichment of gel particles, with $\text{EF} > 1.2$, for both abundance and total area were generally found at wind speed $2\text{-}6 \text{ ms}^{-1}$ (Table 2), except for day 15 on which high CSP

enrichment in the SML ($EF_{Abundance}=4.10$ and $EF_{Total\ area}=3.20$) was observed at wind speed of 18ms^{-1} . Although the median of EF's were significantly lower at wind speed $>6\text{ ms}^{-1}$ than at wind speed $2-6\text{ ms}^{-1}$ ($p<0.05$; two-sample *Kolmogorov-Smirnov test*) (Table 2) gel particles were not always depleted in the SML at high wind speeds. Enrichment of both CSP and TEP at low wind speed was higher for total area than for abundance (Table 2), suggesting selective enrichment of larger gel particles in the SML.

3.3 TEP and CSP size distributions related to wind speeds

The power law relation fitted the gel particles size distribution (d_p : $2-16\text{ }\mu\text{m}$) very well for both CSP_{SML} and TEP_{SML} under different wind speed conditions (mean of $r^2=0.95$) (Fig.4 and Fig.5, slope (δ) data in the SML are given in the supplementary material). The slopes of size distributions for TEP_{SML} ranged from -2.93 to -1.32 (median of -2.17 , $n=16$) at low and moderate wind speeds ($<8\text{ms}^{-1}$) and were significantly higher than those at high speeds ($>8\text{ms}^{-1}$) ranging from -4.05 to -2.39 (median of -3.11 , $n=9$) ($p < 0.05$; two-sample *Kolmogorov-Smirnov test*), excluding samples in the SML collected from day 15 and day 11. Moreover, 8 ms^{-1} was the threshold below which an obvious increase of maximal gel particle size in the SML was found except for day 15. The response of CSP_{SML} slopes to the wind speed varied over time of the experiment. From day 2 to day 11, the slopes of CSP_{SML} were significantly lower at high wind speed ($>8\text{ ms}^{-1}$) (-3.78 to -3.05 , median of -3.28 , $n=8$) than at $<8\text{ ms}^{-1}$ (-3.25 to -2.41 , median of -2.63 , $n=12$) ($p<0.001$; two sample-*Kolmogorov-Smirnov test*). However, during the second part of the experiment, when a seed culture of *E. huxleyi* was added on day 20, followed by a biogenic SML from a previous experiment on day 21, no significant difference of CSP_{SML} size distribution was observed between high and low wind speeds ($p=0.51$, two sample-*Kolmogorov-Smirnov test*), and the negative effect of increasing

wind on the maximum size for CSP_{SML} was less obvious (Fig.6). In addition, the δ values for CSP_{SML} and TEP_{SML} became higher after the addition of the *E. huxleyi* culture. The average slope increased from -2.94 before to -2.37 for CSP_{SML} and from -2.79 before to -2.16 for TEP_{SML} (Fig.7).

Size distribution of gel particles (dp : 2-16 μ m) in the bulk water also followed the power law relationship of Eq. (1) (mean of $r^2=0.99$), with δ varying between -3.48 and -1.94 (mean value: -2.56, SD: 0.49) for TEP_{Bulk} and between -3.43 and -2.01 (mean value:-2.50, SD: 0.42) for CSP_{Bulk} . For the slopes of size distribution in the bulk water, no significant difference was observed between high and low wind speeds. However, as observed for the SML, the δ values of both TEP and CSP in the bulk water were higher after adding the seed culture of *E. huxleyi* on day 20 and a biogenic SML from a previous experiment on day 21 (Fig.7) ($p < 0.05$, two sample-Kolmogorov-Smirnov test), i.e., the average slope of CSP_{Bulk} in size of 2-16 μ m was -2.84 before and -2.15 after addition of the *E. huxleyi* culture.

The abundance of submicron gel particles (0.4-1 μ m) in the SML were analysed at low wind (LW) and high wind (HW) (Fig. S2), respectively. The results showed that the fraction of submicron gel particles became larger at high speed ($>6.1 \text{ ms}^{-1}$) during the period after addition of *E. huxleyi* followed by a biogenic SML from a previous experiment ($p=0.003$ for TEP_{SML} , $p=0.02$ for CSP_{SML} , two sample-Kolmogorov-Smirnov test). The median abundance fraction of submicron gel increased from 33.7% at low to 43.0% at high wind speed for TEP_{SML} and from 38.5% to 46.0% for CSP_{SML} , respectively. There was no enhancement found in submicron fraction at high wind speed before the addition of *E. huxleyi*, with the exception of day 11 when the fraction of submicron TEP_{SML} increased from 37.7% at 3.93 ms^{-1} to 51.4% at 18.2 ms^{-1} .

4 Discussion

4.1 TEP and CSP in SML related to wind speed

The observed differences in concentration, enrichment factor and PSD in response to changes in wind speed revealed that wind speed was an important factor controlling the accumulation of gel particles in the SML during the Aeolotron experiment. Similar results were observed during previous studies, which showed that TEP and particulate organic matter concentrations in SML were negatively related to wind speed (Wurl et al., 2011; Liu and Dickhut, 1998). Initial advection generated at wind speeds of 2-3 ms^{-1} , maintain or enhance enrichments by increasing fluxes of potential microlayer materials to surfaces (Van Vleet and Williams, 1983). As wind speed increases further (4-6 ms^{-1}), micro-scale wave breaking is likely to increase the turbulence in the top surface layer, but does not cause homogenous mixing (Melville, 1996). The contribution of fraction of submicron gels particles became increasing when wind speed was above 6 ms^{-1} , but the threshold of significant changing PSD in SML was wind speed of 8 ms^{-1} . Thus, there is inharmonic effect of wind speeds on the submicron fraction and PSD. For higher wind speeds of 8 ms^{-1} and above, the enhancement of shear and of kinetic energy dissipation by the release of momentum from the wave breaking (Donelan, 2013) were sufficiently energetic to bring about surface disruption and could result in more break-up of gel aggregates and changing PSD of gel particles. Our results on the impact of wind speed on gel particles PSD corroborates earlier findings of Mari and Robert (2008). Aggregation processes are primarily driven by collision rates between particles that depend on particles concentration and turbulent shear (Ellis et al., 2004; Mccave, 1984; Mari and Robert, 2008). It has been suggested that TEP volume concentration increases continuously under the low turbulence intensity by promoting the formation of TEP, but that TEP volume concentration and the fraction of large TEP are reduced at stronger shear (Mari and Robert,

2008). Thus, the effect of wind shear on gel aggregation is double-edged, and large aggregates may be broken apart when the turbulence intensity increases. Our study suggests that high wind speed leads to a break-up of larger gel particles, enhancing the fraction of submicron gels in the SML.

The results of this study indicate that the decrease of total TEP_{SML} area with increasing wind speed may be related to turbulent kinetic energy dissipation ε ($\text{cm}^2 \text{s}^{-3}$). The relationship between gel concentration and turbulence has been reported to be of an exponential form: $e^{(\varepsilon^{1/2})}$ (Ruiz and Izquierdo, 1997). Therefore, increasing kinetic energy dissipation, which is a linear combination of wind speed, wave and buoyancy forcing within the mixed layer (Belcher et al., 2012), likely induces an exponential decrease in the total area of gels in the SML. However, an exponential relationship was not observed between abundance of gel particles and wind speed in this study. A likely explanation is that the abundance of gel particles was influenced not only by turbulence levels, but also by bubble scavenging and bursting at higher speed. In particular small particles that contribute more to total abundance than to total area can accumulate in the SML due to bubble scavenging at high wind speed. This may explain why changes in gel particles abundance did not fit well to an exponential function with wind speed in our study.

According to our results, the average slopes showed about 41.2% changes for TEP_{SML} at speed $> 8 \text{ ms}^{-1}$ compared to low wind speed, but only 23.8% for CSP_{SML} . The change in slope of size distribution between high and low wind speeds was thus higher for TEP_{SML} than CSP_{SML} . In addition, after adding the *E. huxleyi* seed culture, no influence of wind speed on slopes of $CSP_{SML(2-16\mu\text{m})}$ was detected. These results indicated that the influence of wind speed on size distribution of gel particles may be more pronounced for TEP_{SML} than for CSP_{SML} (Prieto et al., 2002; Engel and Galgani, 2016).

2 **4.2 Implication of gel particles in the SML**

3 At lower wind speed, EF's of gel particles in the SML were higher for total area than for
4 abundance. This suggests that large gel particles became selectively enriched in the SML and,
5 due to their larger surface area, may act as a cover sheet, potentially impacting processes
6 across the air-sea interface at low wind speeds. Based on the data from the Aeolotron
7 experiment, a schematic diagram on interactions between physical dynamics and gel particle
8 coverage in the SML is proposed (Fig. 8): The enrichment of TEP and CSP in the SML
9 existed until wind speed reached 6 ms^{-1} , with strong enrichment at about $2\text{-}4 \text{ ms}^{-1}$, at which
10 slick streaks and bands were observed visually. Although surface tension measurements were
11 not made, values for the mean square slope, a measurement of surface roughness, were two or
12 three orders of magnitude higher at wind speeds $> 6 \text{ ms}^{-1}$ than at wind speeds $< 6 \text{ ms}^{-1}$
13 (Maximilian Bopp and Bernd Jähne, personal communication). At wind speed of 8 ms^{-1} the
14 sea surface became rougher and wave breaking started. In consequence, the SML started to
15 mix with the subsurface water leading to a more homogeneous distribution of matter in the
16 surface water column and a potential role of gel particles in gas-exchange would be reduced.

17 Under conditions of high wind and wave breaking, submicron gels can be aerosolized with
18 sea spray (Gantt et al., 2011). For the ocean, gel particle emission in aerosols has recently
19 been discussed with respect to cloud formation, precipitation, the hydrological cycle, and
20 climate (Knopf et al., 2011; Wilson et al., 2015; Alpert et al., 2011). In this study, we found
21 that the fraction of submicron gels ($0.4\text{-}1\mu\text{m}$) in the SML increased at high wind speeds (>6
22 ms^{-1}) after the addition of *E. huxleyi* and on day 11 with the peak concentration of bacterial
23 abundance in SML (Fig 8). Due to the TEP's flexible nature, small gels can pass through a
24 filter with size of $0.4 \mu\text{m}$ (Passow and Alldredge, 1995) and thus may escape the

measurement. It is therefore likely that the fraction of submicron gels was even higher at high wind speeds than observed. The changes of size distribution of gel particles in SML indicated that large gel particles were fragmented into smaller gels at high wind speed, or that submicron gels were generated. Strong enrichment of TEP in submicron SSA under field conditions has been observed by Aller et al. (2017). Production of SSA in the field is driven by wind speed, and SSA in the size range 0.4-1 μm in particular were observed to be higher at high wind speed (Lehahn et al., 2014). Therefore, our finding supported the results of Aller et al (2017) and Lehahn et al (2014) and suggest that the enhanced contribution of submicron gels particle at higher wind $>6\text{ms}^{-1}$ after the addition of *E. huxleyi*, potentially impact the emission of gels with sea spray aerosol.

In addition, pronounced changes through time in gel size slope and EF's were observed after the addition of *E. huxleyi* seed culture. At that time, shallower slopes for CSP and TEP revealed a higher abundance of larger gel particles relative to smaller ones for both SML and bulk water. Gel particles produced by autotrophs may be more surface active and more prone to aggregation (Zhou et al., 1998). The larger particle combined with the ballast effect of *E. huxleyi* are more easily to sink out of the SML. This, to a certain extent, may explain that a decrease in the EF's of CSP and TEP after the addition of the *E. huxleyi* seed. The observed changes after addition of the *E. huxleyi* seed culture indicates that variations of gel particles in the SML may also depend on the source of gels and gel precursors.

5 Conclusion

Our study showed that an enrichment of biogenic gel particles in SML can occur at low speed ($< 6 \text{ ms}^{-1}$) despite low autotrophic productivity in the water column. A negative exponential relationship between the total area of gel particles in the SML and wind speed was observed in most cases. Our results showed that the PSD is an important parameter for characterizing

1 the shape of the gel particle size distribution in the SML and reflects the particles' fate in the
2 SML (i.e. aggregation, fragmentation and injecting into air). The slope of PSD for TEP_(2-16μm)
3 and the maximum size of gel particles in the SML varied significantly at about 8 ms⁻¹. The
4 influence of wind speed on spectral slopes is more pronounced for TEP_{SML} than for CSP_{SML},
5 and that CSP_{SML} are less prone to aggregation than TEP_{SML} during the low wind speed. The
6 enhancement of contribution of submicron gels particle in the SML at higher wind (> 6ms⁻¹)
7 after the addition of *E. huxleyi* indicate that biological activity may potentially influence the
8 emission of gels with sea spray aerosol. Overall, variations of gel particles sizes in the SML
9 can provide useful information on particle dynamics at the interface between air and sea.

10 To better understand the role of biogenic gel particles for bio-physico-chemical processes
11 across the air-sea interface, future studies should consider the full size spectrum of gels
12 scaling from nanometers to micrometers and also include their chemical composition. This
13 could provide important information on implications of marine gels for the aerosol and cloud
14 formation as well as for air-sea gas exchange.

16 **Data availability**

17 All data will become available at [https://doi.pangaea.de/upon publication](https://doi.pangaea.de/upon%20publication).

21 **Competing interest**

22 The authors declare that they have no conflict of interest.

1

2 **Acknowledgements**

3 We thank Tania Klüver, Ruth Flerus, Katja Laß, Sonja Endres and Jon Roa for technical
4 assistance. Armin Form helped to collect seawater for the Aeolotron experiment onboard of
5 the *RV Poseidon*. This study was supported by the SOPRANIII project (03F06622.2) and by
6 China Scholarship Council (grant number 201408440016). We also thank Bernd Jähne,
7 Kerstin Krall and Maximilian Bopp for providing access and support during the Aeolotron
8 experiment, and for sharing their data and knowledge. This study is a contribution to the
9 international Surface Ocean Lower Atmosphere Study (SOLAS).

10

References

- Allredge, A. L., Passow, U., and Logan, B. E.: The Abundance and Significance of a Class of Large, Transparent Organic Particles in the Ocean, *Deep-Sea Res Pt I*, 40, 1131-1140, Doi 10.1016/0967-0637(93)90129-Q, 1993.
- Aller, J. Y., Radway, J. C., Kilthau, W. P., Bothe, D. W., Wilson, T. W., Vaillancourt, R. D., Quinn, P. K., Coffman, D. J., Murray, B. J., and Knopf, D. A.: Size-resolved characterization of the polysaccharidic and proteinaceous components of sea spray aerosol, *Atmos Environ*, 154, 331-347, <https://doi.org/10.1016/j.atmosenv.2017.01.053>, 2017.
- Alpert, P. A., Aller, J. Y., and Knopf, D. A.: Initiation of the ice phase by marine biogenic surfaces in supersaturated gas and supercooled aqueous phases, *Phys Chem Chem Phys*, 13, 19882-19894, 10.1039/c1cp21844a, 2011.
- Azetsu-Scott, K., and Passow, U.: Ascending marine particles: Significance of transparent exopolymer particles (TEP) in the upper ocean, *Limnol Oceanogr*, 49, 741-748, 2004.
- Azetsu-Scott, K., and Niven, S. E. H.: The role of transparent exopolymer particles (TEP) in the transport of Th-234 in coastal water during a spring bloom, *Cont Shelf Res*, 25, 1133-1141, 10.1016/j.csr.2004.12.013, 2005.
- Baeza, R., Carrera Sanchez, C., Pilosof, A. M. R., and Rodríguez Patino, J. M.: Interactions of polysaccharides with β -lactoglobulin adsorbed films at the air-water interface, *Food Hydrocolloids*, 19, 239-248, <http://dx.doi.org/10.1016/j.foodhyd.2004.06.002>, 2005.
- Belcher, S. E., Grant, A. L. M., Hanley, K. E., Fox-Kemper, B., Van Roekel, L., Sullivan, P. P., Large, W. G., Brown, A., Hines, A., Calvert, D., Rutgersson, A., Pettersson, H., Bidlot, J. R., Janssen, P. A. E. M., and Polton, J. A.: A global perspective on Langmuir turbulence in the ocean surface boundary layer, *Geophys Res Lett*, 39, Art. L18605, 10.1029/2012gl052932, 2012.
- Bopp, M., and Jähne, B.: Measurements of the friction velocity in a circular wind-wave tank by the momentum balance method, Unpublished, 2014.
- Calleja, M. L., Duarte, C. M., Prairie, Y. T., Agusti, S., and Herndl, G. J.: Evidence for surface organic matter modulation of air-sea CO₂ gas exchange, *Biogeosciences*, 6, 1105-1114, 2009.
- Carlson, D. J.: Dissolved Organic Materials in Surface Microlayers - Temporal and Spatial Variability and Relation to Sea State, *Limnology and Oceanography*, 28, 415-431, 1983.
- Cunliffe, M., Engel, A., Frka, S., Gasparovic, B., Guitart, C., Murrell, J. C., Salter, M., Stolle, C., Upstill-Goddard, R., and Wurl, O.: Sea surface microlayers: A unified physicochemical and biological perspective of the air-ocean interface, *Prog Oceanogr*, 109, 104-116, 10.1016/j.pocean.2012.08.004, 2013.
- Dickinson, E.: Hydrocolloids at interfaces and the influence on the properties of dispersed systems, *Food Hydrocolloid*, 17, 25-39, Pii S0268-005x(01)00120-5, Doi 10.1016/S0268-005x(01)00120-5, 2003.
- Donelan, M. A.: Air-Water Exchange Processes, in: *Physical Processes in Lakes and Oceans*, American Geophysical Union, 19-36, 2013.

1 Ebling, A. M., and Landing, W. M.: Sampling and analysis of the sea surface microlayer for
2 dissolved and particulate trace elements, *Mar Chem*, 177, 134-142,
3 10.1016/j.marchem.2015.03.012, 2015.

4 Ellis, K. M., Bowers, D. G., and Jones, S. E.: A study of the temporal variability in particle
5 size in a high energy regime, *Coast. Shelf Sci.*, 61, 311-315, 2004.

6 Engel, A., Thoms, S., Riebesell, U., Rochelle-Newall, E., and Zondervan, I.: Polysaccharide
7 aggregation as a potential sink of marine dissolved organic carbon, *Nature*, 428, 929-932,
8 10.1038/nature02453, 2004.

9 Engel, A.: Determination of marine gel particles. Practical Guidelines for the Analysis of
10 Seawater, , 2009.

11 Engel, A., and Galgani, L.: The organic sea-surface microlayer in the upwelling region off the
12 coast of Peru and potential implications for air-sea exchange processes, *Biogeosciences*, 13,
13 989-1007, 10.5194/bg-13-989-2016, 2016.

14 Engel, A., Sperling, M., Sun, C.C, Grosse, J. and Friedrichs, G. Bacterial control of organic
15 matter in the surface microlayer: Insights from a wind wave channel experiment. *Frontiers in*
16 *Marine Sciences*, submitted.

17 Falkowska, L.: a field evaluation of teflon plate, glass plate and screen sampling techniques.
18 Part 1. Thickness of microlayer samples and relation to wind speed. In: *Oceanol. Acta*, 1999.

19 Frew, N. M., Bock, E. J., Schimpf, U., Hara, T., Haussecker, H., Edson, J. B., McGillis, W. R.,
20 Nelson, R. K., McKenna, S. P., Uz, B. M., and Jahne, B.: Air-sea gas transfer: Its dependence
21 on wind stress, small-scale roughness, and surface films, *J Geophys Res-Oceans*, 109, 2004.

22 Gantt, B., Meskhidze, N., Facchini, M. C., Rinaldi, M., Ceburnis, D., and O'Dowd, C. D.:
23 Wind speed dependent size-resolved parameterization for the organic mass fraction of sea
24 spray aerosol, *Atmos Chem Phys*, 11, 8777-8790, 10.5194/acp-11-8777-2011, 2011.

25 Gao, Q., Leck, C., Rauschenberg, C., and Matrai, P. A.: On the chemical dynamics of
26 extracellular polysaccharides in the high Arctic surface microlayer, *Ocean Sci*, 8, 401-418,
27 10.5194/os-8-401-2012, 2012.

28 Garrett, W. D., and Duce, R. A.: Surface Microlayer Samplers, in: *Air-Sea Interaction:*
29 *Instruments and Methods*, edited by: Dobson, F., Hasse, L., and Davis, R., Springer US,
30 Boston, MA, 471-490, 1980.

31 GESAMP: The Sea-Surface Microlayer and its Role in Global Change. Reports and Studies,
32 WMO, 1995.

33 Graham, D. E., and Phillips, M. C.: Proteins at liquid interfaces: I. Kinetics of adsorption and
34 surface denaturation, *J Colloid Interf Sci*, 70, 403-414, [https://doi.org/10.1016/0021-](https://doi.org/10.1016/0021-9797(79)90048-1)
35 [9797\(79\)90048-1](https://doi.org/10.1016/0021-9797(79)90048-1), 1979.

36 Guasco, T. L., Cuadra-Rodriguez, L. A., Pedler, B. E., Ault, A. P., Collins, D. B., Zhao, D. F.,
37 Kim, M. J., Ruppel, M. J., Wilson, S. C., Pomeroy, R. S., Grassian, V. H., Azam, F., Bertram,
38 T. H., and Prather, K. A.: Transition Metal Associations with Primary Biological Particles in
39 Sea Spray Aerosol Generated in a Wave Channel, *Environ Sci Technol*, 48, 1324-1333,
40 10.1021/es403203d, 2014.

41 Knopf, D. A., Alpert, P. A., Wang, B., and Aller, J. Y.: Stimulation of ice nucleation by
42 marine diatoms, *Nature Geoscience*, 4, 88-90, <http://dx.doi.org/10.1038/ngeo1037>, 2011.

1 Kuhnhenh-Dauben, V., Purdie, D. A., Knispel, U., Voss, H., and Horstmann, U.: Effect of
2 phytoplankton growth on air bubble residence time in seawater, *J Geophys Res-Oceans*, 113,
3 2008.

4 Kuznetsova, M., Lee, C., and Aller, J.: Characterization of the proteinaceous matter in marine
5 aerosols, *Mar Chem*, 96, 359-377, 10.1016/j.marchem.2005.03.007, 2005.

6 Leck, C., and Bigg, E. K.: Source and evolution of the marine aerosol - A new perspective,
7 *Geophys Res Lett*, 32, 2005.

8 Lehahn, Y., Koren, I., Rudich, Y., Bidle, K. D., Trainic, M., Flores, J. M., Sharoni, S., and
9 Vardi, A.: Decoupling atmospheric and oceanic factors affecting aerosol loading over a
10 cluster of mesoscale North Atlantic eddies, *Geophys Res Lett*, 41, 4075-4081,
11 10.1002/2014GL059738, 2014.

12 Liss, P. S. a. D., R. A.: *The Sea Surface and Global Change*, Cambridge University Press,
13 2005.

14 Liu, K. W., and Dickhut, R. M.: Effects of wind speed and particulate matter source on
15 surface microlayer characteristics and enrichment of organic matter in southern Chesapeake
16 Bay, *J Geophys Res-Atmos*, 103, 10571-10577, Doi 10.1029/97jd03736, 1998.

17 Long, R. A., and Azam, F.: Abundant protein-containing particles in the sea, *Aquat Microb*
18 *Ecol*, 10, 213-221, Doi 10.3354/Ame010213, 1996.

19 Mari, X., and Kiorboe, T.: Abundance, size distribution and bacterial colonization of
20 transparent exopolymeric particles (TEP) during spring in the Kattegat, *J Plankton Res*, 18,
21 969-986, DOI 10.1093/plankt/18.6.969, 1996.

22 Mari, X., and Robert, M.: Metal induced variations of TEP sticking properties in the
23 southwestern lagoon of New Caledonia, *Mar Chem*, 110, 98-108, 2008.

24 Mari, X., Passow, U., Migon, C., Burd, A. B., and Legendre, L.: Transparent exopolymer
25 particles: Effects on carbon cycling in the ocean, *Prog Oceanogr*, 151, 13-37,
26 <http://dx.doi.org/10.1016/j.pocean.2016.11.002>, 2017.

27 McCave, I. N.: Size Spectra and Aggregation of Suspended Particles in the Deep Ocean,
28 *Deep-Sea Res*, 31, 329-352, Doi 10.1016/0198-0149(84)90088-8, 1984.

29 Melville, W. K.: The role of surface-wave breaking in the air-sea interaction, *Annu. Rev.*
30 *Fluid Mech.*, 28, 279-321, 1996.

31 Mesarchaki, E., Krauter, C., Krall, K. E., Bopp, M., Helleis, F., Williams, J., and Jahne, B.:
32 Measuring air-sea gas-exchange velocities in a large-scale annular wind-wave tank, *Ocean Sci*,
33 11, 121-138, 10.5194/os-11-121-2015, 2015.

34 Mopper, K., Zhou, J. A., Ramana, K. S., Passow, U., Dam, H. G., and Drapeau, D. T.: The
35 Role of Surface-Active Carbohydrates in the Flocculation of a Diatom Bloom in a Mesocosm,
36 *Deep-Sea Res Pt II*, 42, 47-73, Doi 10.1016/0967-0645(95)00004-A, 1995.

37 Nagel, L., Krall, K. E., and Jahne, B.: Comparative heat and gas exchange measurements in
38 the Heidelberg Aeolotron, a large annular wind-wave tank, *Ocean Sci*, 11, 111-120,
39 10.5194/os-11-111-2015, 2015.

40 Oppo, C., Bellandi, S., Innocenti, N. D., Stortini, A. M., Loglio, G., Schiavuta, E., and Cini,
41 R.: Surfactant components of marine organic matter as agents for biogeochemical
42 fractionation and pollutant transport via marine aerosols, *Mar Chem*, 63, 235-253, Doi
43 10.1016/S0304-4203(98)00065-6, 1999.

1 Orellana, M. V., Matrai, P. A., Leck, C., Rauschenberg, C. D., Lee, A. M., and Coz, E.:
2 Marine microgels as a source of cloud condensation nuclei in the high Arctic, *P Natl Acad Sci*
3 *USA*, 108, 13612-13617, 10.1073/pnas.1102457108, 2011.

4 Passow, U., and Alldredge, A. L.: Aggregation of a Diatom Bloom in a Mesocosm - the Role
5 of Transparent Exopolymer Particles (Tep), *Deep-Sea Res Pt II*, 42, 99-109, Doi
6 10.1016/0967-0645(95)00006-C, 1995.

7 Passow, U.: Transparent exopolymer particles (TEP) in aquatic environments, *Prog Oceanogr*,
8 55, 287-333, Doi 10.1016/S0079-6611(02)00138-6, 2002.

9 Patino, J. M. R., and Pilosof, A. M. R.: Protein-polysaccharide interactions at fluid interfaces,
10 *Food Hydrocolloid*, 25, 1925-1937, 10.1016/j.foodhyd.2011.02.023, 2011.

11 Prieto, L., Ruiz, J., Echevarria, F., Garcia, C. M., Bartual, A., Galvez, J. A., Corzo, A., and
12 Macias, D.: Scales and processes in the aggregation of diatom blooms: high time resolution
13 and wide size range records in a mesocosm study, *Deep-Sea Res Pt I*, 49, 1233-1253, 2002.

14 Romano, J. C.: Sea-surface slick occurrence in the open sea (Mediterranean, Red Sea, Indian
15 Ocean) in relation to wind speed, *Deep-Sea Res Pt I*, 43, 411-423, Doi 10.1016/0967-
16 0637(96)00024-6, 1996.

17 Ruiz, J. E., and Izquierdo, A.: A simple model for the break-up of marine aggregates by
18 turbulent shear, *Oceanologica Acta*, 20, 597-605, 1997.

19 Russell, L. M., Hawkins, L. N., Frossard, A. A., Quinn, P. K., and Bates, T. S.: Carbohydrate-
20 like composition of submicron atmospheric particles and their production from ocean bubble
21 bursting, *P Natl Acad Sci USA*, 107, 6652-6657, 10.1073/pnas.0908905107, 2010.

22 Stoderegger, K. E., and Herndl, G. J.: Production of exopolymer particles by marine
23 bacterioplankton under contrasting turbulence conditions, *Marine Ecology Progress*, 189, 9-
24 16, 1999.

25 Thorpe, S. A., Bowyer, P., and Woolf, D. K.: Some Factors Affecting the Size Distributions
26 of Oceanic Bubbles, *J Phys Oceanogr*, 22, 382-389, 1992.

27 UNESCO: Procedur for sampling the sea surface microlaye, in: *IOC Manuals and Guide 15*,
28 Paris, 1985.

29 Van Vleet, E. S., and Williams, P. M.: Surface potential and film pressure measurements in
30 seawater systems1, *Limnol Oceanogr*, 28, 401-414, 10.4319/lo.1983.28.3.0401, 1983.

31 Wilson, T. W., Ladino, L. A., Alpert, P. A., Breckels, M. N., Brooks, I. M., Browse, J.,
32 Burrows, S. M., Carslaw, K. S., Huffman, J. A., Judd, C., Kilthau, W. P., Mason, R. H.,
33 McFiggans, G., Miller, L. A., Najera, J. J., Polishchuk, E., Rae, S., Schiller, C. L., Si, M.,
34 Temprado, J. V., Whale, T. F., Wong, J. P. S., Wurl, O., Yakobi-Hancock, J. D., Abbatt, J. P.
35 D., Aller, J. Y., Bertram, A. K., Knopf, D. A., and Murray, B. J.: A marine biogenic source of
36 atmospheric ice-nucleating particles, *Nature*, 525, 234+, 10.1038/nature14986, 2015.

37 Wurl, O., and Holmes, M.: The gelatinous nature of the sea-surface microlayer, *Mar Chem*,
38 110, 89-97, 10.1016/j.marchem.2008.02.009, 2008.

39 Wurl, O., Miller, L., Ruttgers, R., and Vagle, S.: The distribution and fate of surface-active
40 substances in the sea-surface microlayer and water column, *Mar Chem*, 115, 1-9,
41 10.1016/j.marchem.2009.04.007, 2009.

42 Wurl, O., Miller, L., and Vagle, S.: Production and fate of transparent exopolymer particles in
43 the ocean, *J Geophys Res-Oceans*, 116, 2011.

1 Wurl, O., Stolle, C., Van Thuoc, C., The Thu, P., and Mari, X.: Biofilm-like properties of the
2 sea surface and predicted effects on air–sea CO₂ exchange, *Prog Oceanogr*, 144, 15-24,
3 <http://dx.doi.org/10.1016/j.pocean.2016.03.002>, 2016.

4 Zhou, J., Mopper, K., and Passow, U.: The role of surface-active carbohydrates in the
5 formation of transparent exopolymer particles by bubble adsorption of seawater, *Limnol*
6 *Oceanogr*, 43, 1860-1871, 1998.

Tables

Table 1: Wind speed settings as applied during strategy I of the Aeolotron experiment;

‘NaN’: no values for U_{10} .

Day	Wind velocity U_{10} (m s ⁻¹)					
2	NaN	NaN	3.98	5.38	11.1	17.9
4	2.09	3.44	4.31	8.31	14.2	
9	1.54	2.40	4.07	5.29	11.1	
11	1.66	2.89	3.93	8.03	14.0	NaN
15	2.58	4.99	6.42	11.1	18.1	
22	1.37	1.37	4.53	6.1	11.3	18.7
24	1.44	2.65	4.27	5.38	11.4	18.1

Table 2: Enrichment factors (EF) for gel particles abundance and total area in the SML at different wind speeds; (EF_{Total area} > EF_{Abundance} are marked bold)

Experiment day	Wind speed (m s ⁻¹)	TEP		CSP	
		EF _{Abundance}	EF _{Total area}	EF _{Abundance}	EF _{Total area}
2	NaN(<4ms⁻¹)	2.24	7.40	41.43	113.98
	17.9	1.80	1.71	8.21	12.27
4	2.09	0.97	5.71	3.52	26.81
9	1.54	3.34	16.16	nd	nd
	2.40	4.80	12.76	1.84	7.08
	5.29	1.44	5.40	1.20	2.78
	11.1	1.08	1.07	0.74	0.72
11	3.93	0.91	1.16	13.46	31.16
	18.2	1.63	1.53	1.11	1.12
15	2.58	1.06	1.13	1.28	1.03
	4.99	0.48	0.77	0.47	1.08
	6.42	0.68	0.95	1.39	2.02
	11.1	0.77	0.70	2.14	1.50
22	18.1	1.28	1.02	4.10	3.20
	1.37	3.06	4.38	1.14	2.41
	4.53	3.06	5.04	5.46	4.54
	6.10	2.94	4.78	1.34	2.23
24	11.3	0.61	1.02	1.07	1.02
	18.7	0.44	0.58	1.41	0.85
	1.44	4.68	8.21	1.82	3.93
	4.27	6.97	6.06	5.94	6.82
	5.38	6.42	5.19	2.44	4.05
	11.4	2.38	1.23	0.72	0.66
Median of EF's	18.1	1.74	0.81	0.65	0.69
	<6ms ⁻¹	3.06	7.81	6.48	19.22
Median of EF's	>6ms ⁻¹	1.28	1.53	2.14	2.23

1 **Figure captions**

2 Figure 1: Schematic wind speed (U_{10}) increase as applied during strategy I for experiments
3 conducted in the Aeolotron.

4 Figure 2: Response of abundance and total area for TEP_{SML} to increasing wind speeds,
5 the error bars indicate ± 1 SD.

6 Figure 3: Response of abundance and total area for CSP_{SML} to increasing wind speeds,
7 the error bars indicate ± 1 SD.

8 Figure 4: PSD of TEP_{SML} at different wind speeds (linear regressions of $\log(dN/d(dp))$ vs.
9 $\log(dp)$ were fitted to particles in the size range of 2-16 μm ESD, with wind speeds $< 8\text{ms}^{-1}$
10 (solid line) and wind speeds $> 8\text{ms}^{-1}$ (dash and dot).

11 Figure 5: PSD of CSP_{SML} at different wind speeds (linear regressions of $\log(dN/d(dp))$ vs.
12 $\log(dp)$ were fitted to particles in the size range of 2-16 μm ESD, with wind speeds $< 8\text{ms}^{-1}$
13 (solid line) and wind speeds $> 8\text{ms}^{-1}$ (dash and dot)).

14 Figure 6, A-D: Maximum size (ESD) of gel particles in the SML; A) and C): before addition
15 of *E. huxleyi*; B) and D): after addition of *E. huxleyi*.

16 Figure 7: Average slopes of gel particles in the bulk water and SML. Open bars: before
17 addition of *E. huxleyi*, hatched bars: after addition of *E. huxleyi*, error bars indicate ± 1 SD.

18 Figure 8, A-G: Strong accumulation of TEP and CSP in the SML at low wind speed as
19 determined by microscopy, A: TEP (2.0 ms^{-1}), B: TEP (4.3 ms^{-1}), C: TEP (8.3 ms^{-1}), D: CSP
20 (2.0 ms^{-1}), E: CSP (4.3 ms^{-1}), F: CSP (8.3 ms^{-1}); G: Proposed schematic for interactions
21 between wind speed and gel particle coverage in the SML.

22

1

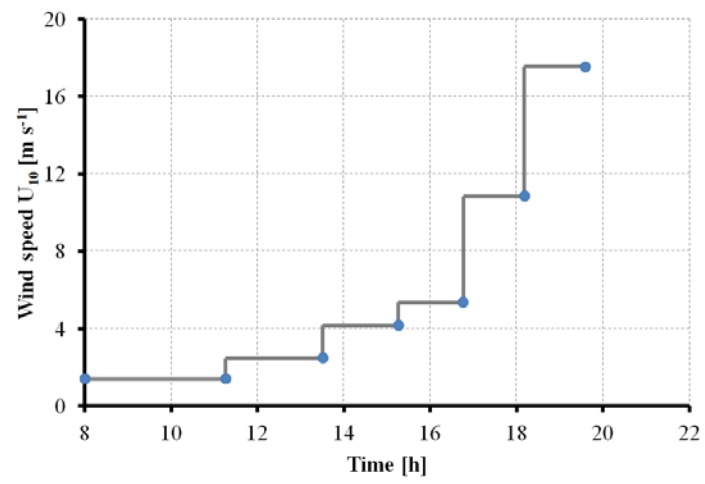


Figure 1

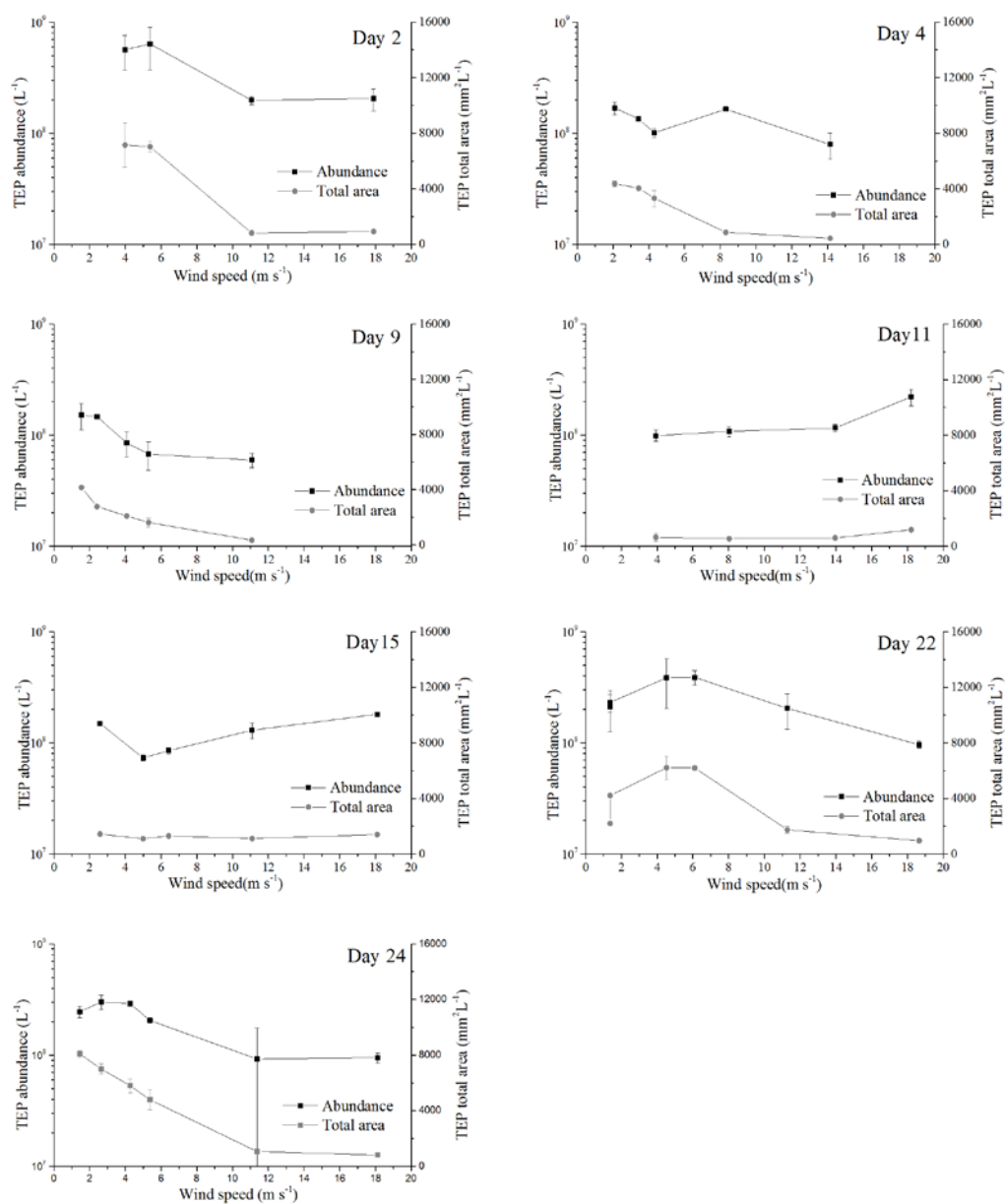
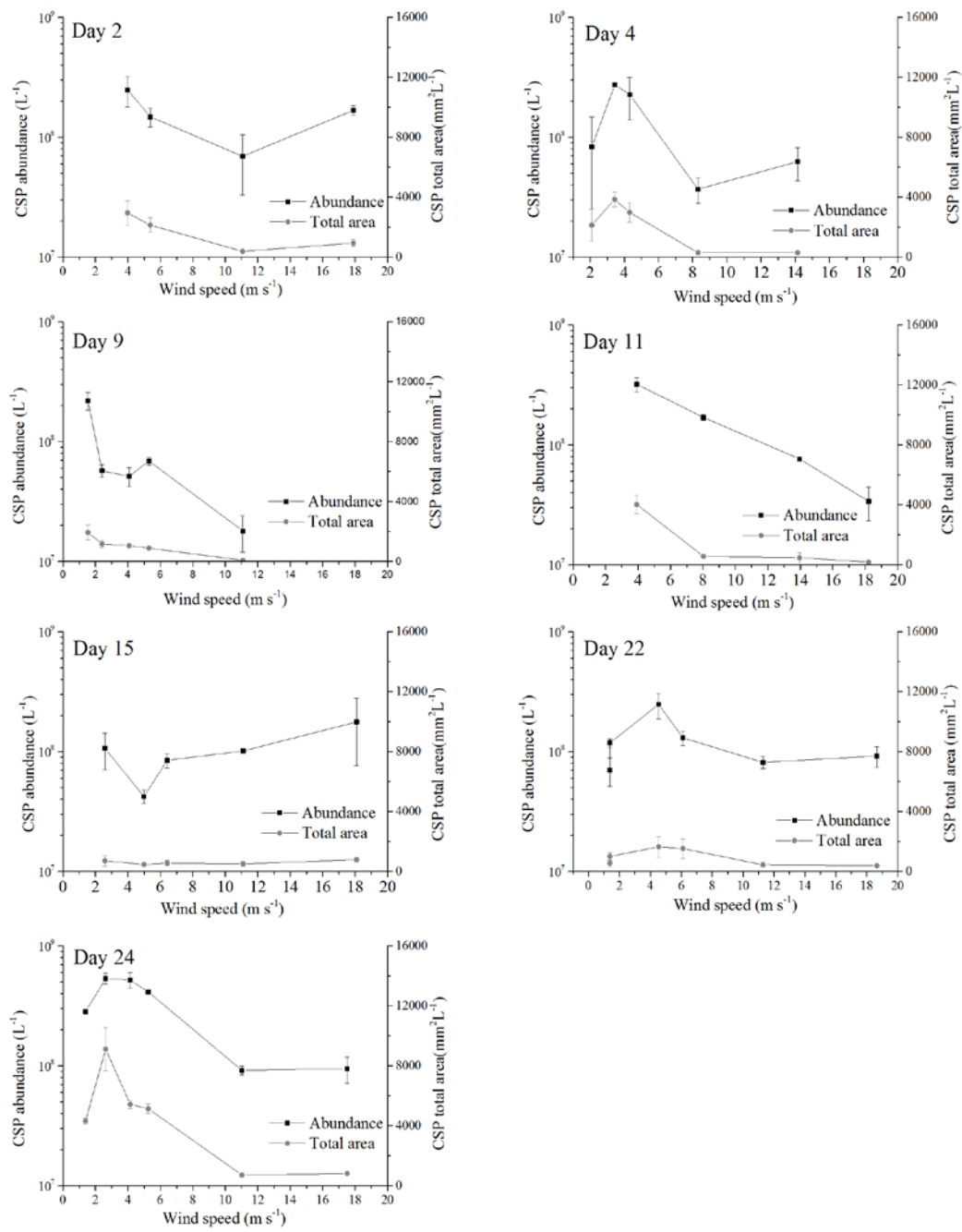


Figure 2

1
2



3
4
5

Figure 3

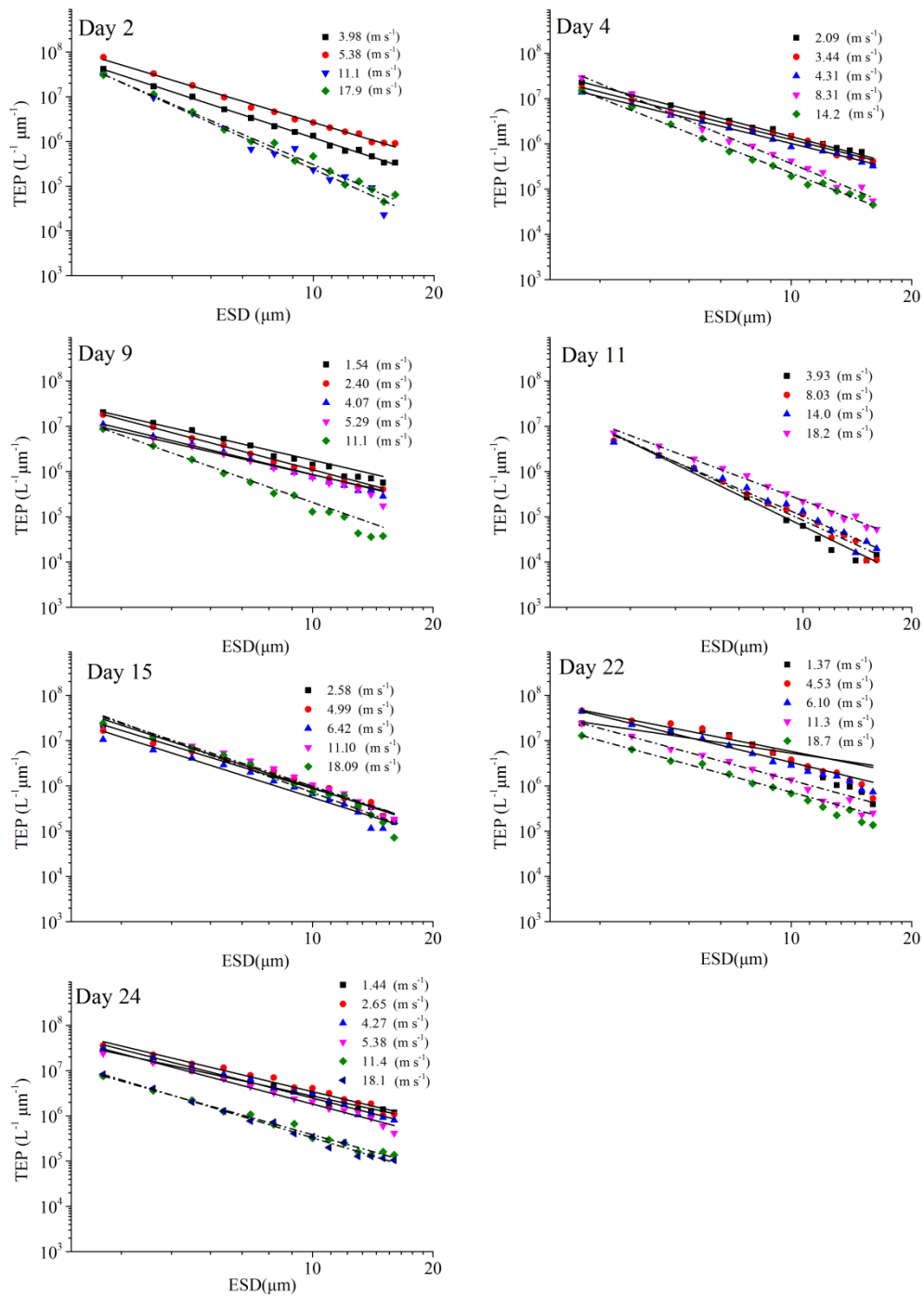


Figure 4

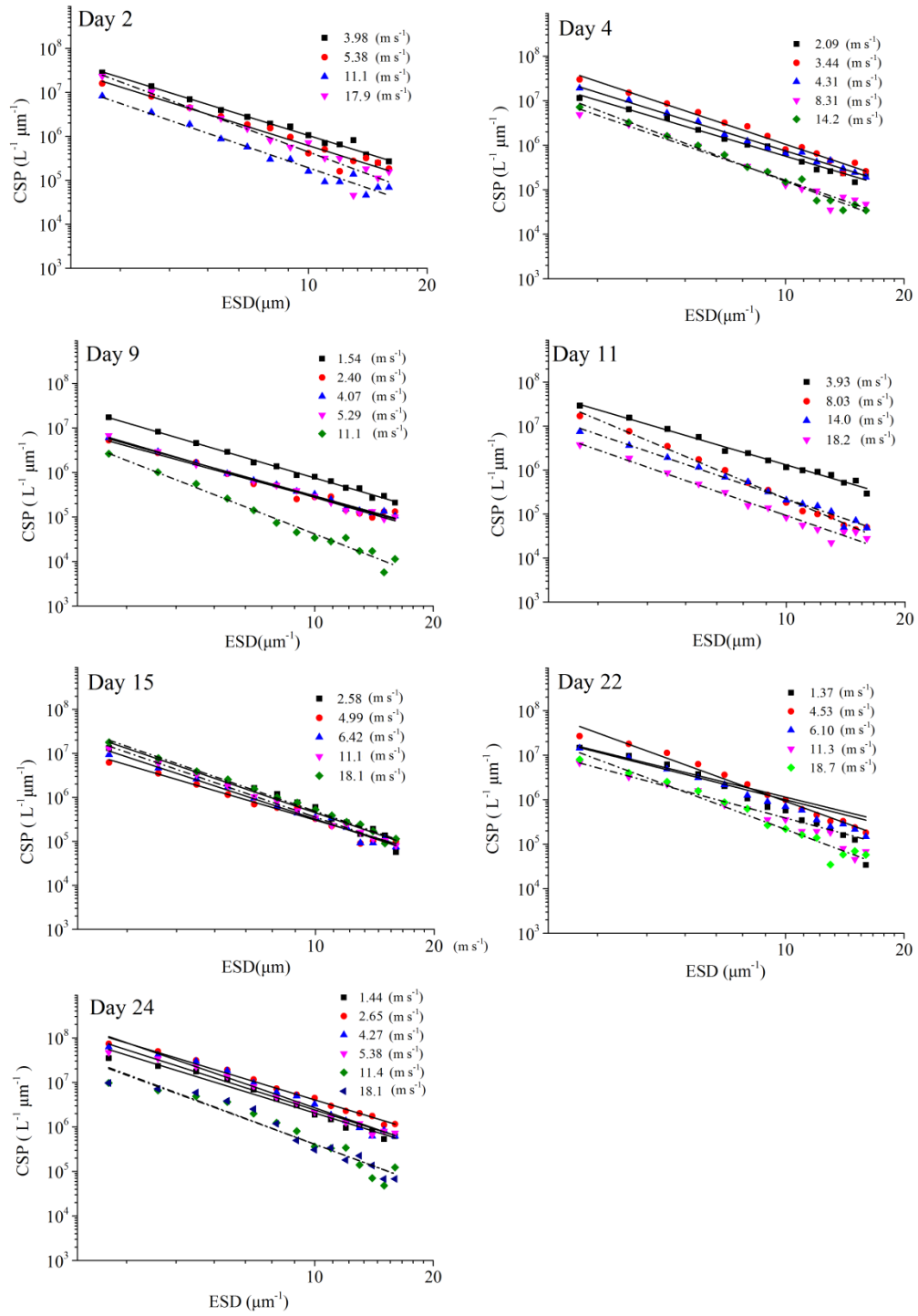


Figure 5

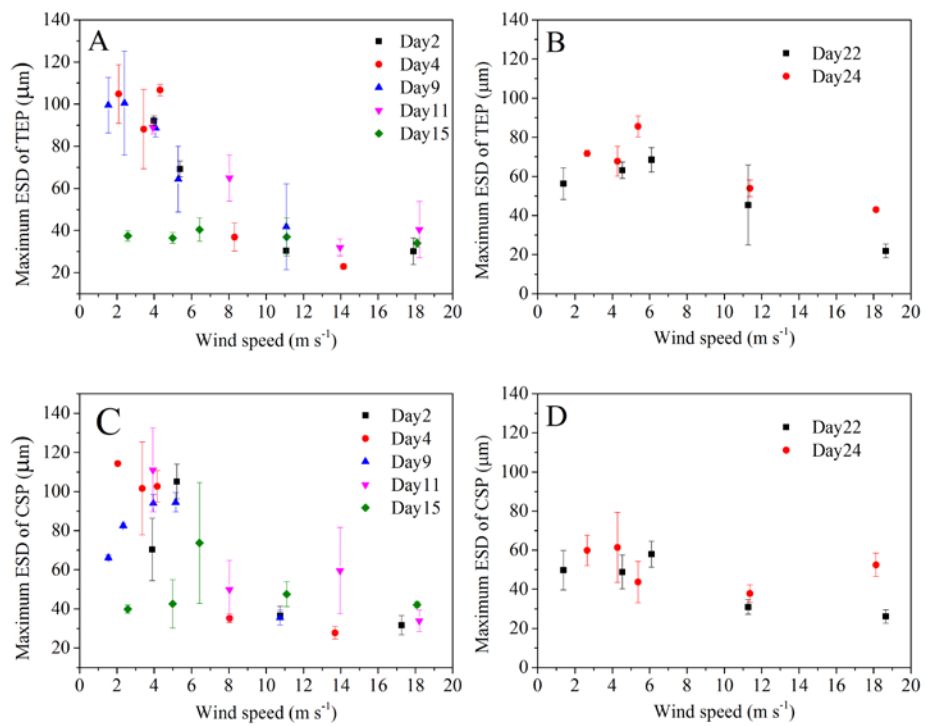


Figure 6

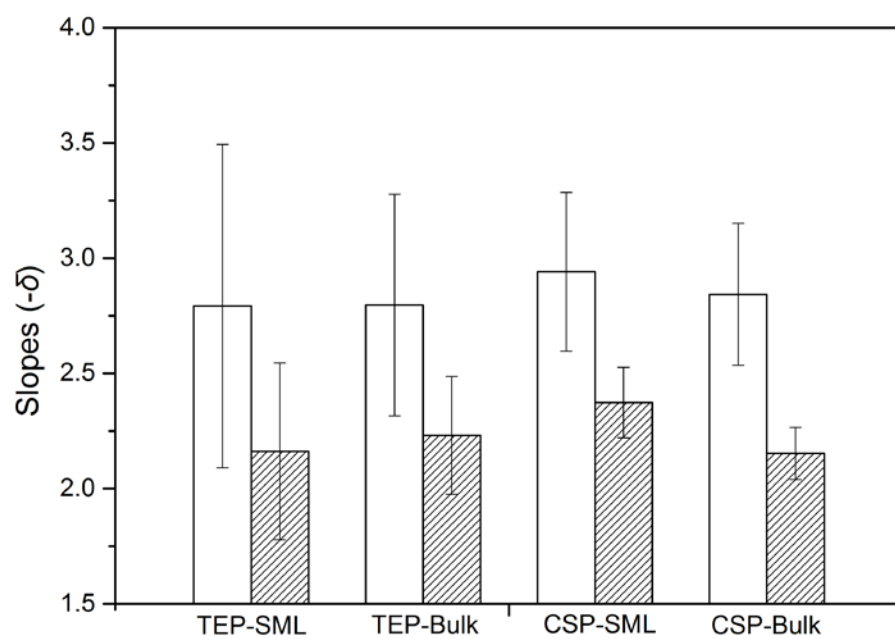


Figure 7

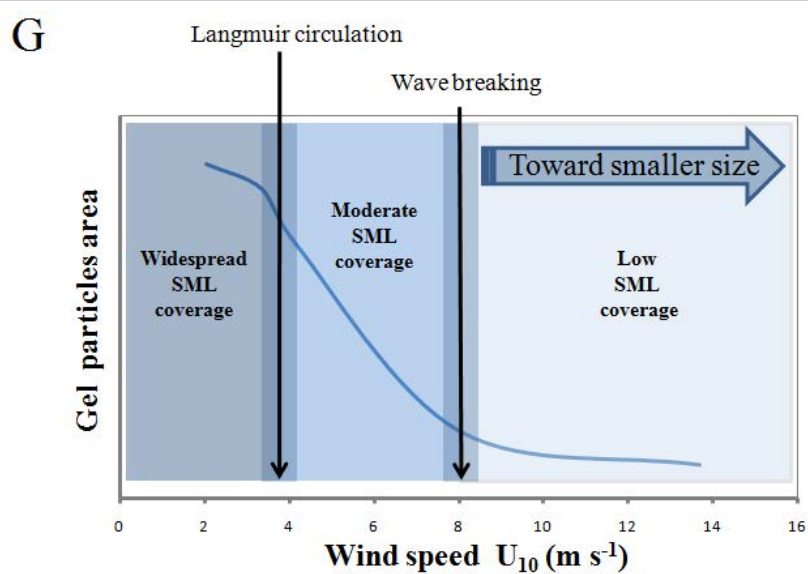
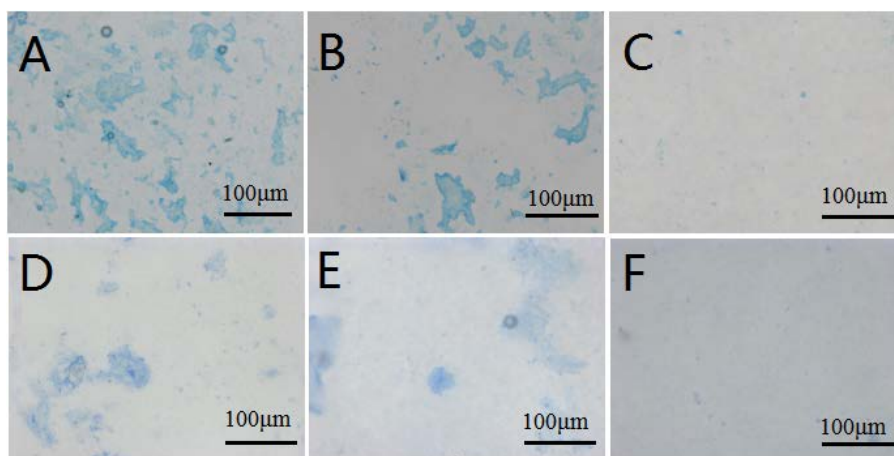


Figure 8